Scientific Journal for Damietta Faculty of Science **14**(2) 2024, 1-12
doi: 10.21608/SJDFS.2024.288167.1166
ISSN Print 2314-8594
ISSN Online 2314-8616

https://sjdfs.journals.ekb.eg/

Protective and Therapeutic Effects of Moringa Oleifera Leave Nanoparticles against Acrylamide-Induced Hepato and Renal Toxicity in Adult Male Rats

Kadry El-Bakry[1], Nahed Omar[1], Lamiaa Deef[1], Shereen Fahmy[1] and Abdullah Yaquob*[2]

[1]Zoology Department, Faculty of Science, Damietta University, Damietta, Egypt.
[2]Zoology Department, Faculty of Science, Sabha University, Sabha, Libya.

Received: 08 May 2024 /Accepted: 06 June 2024

*Corresponding author's E-mail: yacoopa@students.du.edu.eg

Abstract

Atriplex species are tolerant to drought and salinity, therefore; they are appropriate for restoration The study investigated the effects of acrylamide (ACR) on the liver and kidneys in rats and the potential protective and therapeutic properties of *Moringa oleifera (M. oleifera*) leaf nanoparticles, using UV-visible spectroscopy to create and characterize silver nanoparticles. 20 adult male rats were randomly divided into four groups: Control group (CT); Acrylamide group (ACR): rats received 50 mg/kg b.wt. in drinking water for 3 weeks; Protection group (Mo-NPs /ACR): rats received 50 mg/kg b.wt. of *M. oleifera* nanoparticles (Mo-NPs) daily for 3 weeks and were given 50 mg/kg b.wt. of acrylamide (ACR) daily for 3 weeks; Treatment group (ACR/Mo-NPs): rats were given 50 mg/kg b.wt. of acrylamide (ACR) for 3 weeks, followed by *M. oleifera* nanoparticles (Mo-NPs) for 3 weeks. Blood and tissue samples were obtained for the physiological and histological investigations, and a comet assay was used to determine the amount of DNA damage. Administration of ACR increased MDA, creatinine, urea, ALT, and AST activities while decreasing SOD enzyme activity. *M. oleifera* nanoparticle treatment raised SOD enzyme activity and decreased the damaging effects of ACR on these levels. Rats with ACR injuries treated with *M. oleifera* nanoparticles had improved histological abnormalities in their liver and kidneys. Greater DNA damage was seen in the liver cells of the ACR group; however, *M. oleifera* nanoparticles may have repaired this damage in other groups. The study concluded that *M. oleifera* nanoparticles provide enhanced protection against ACR's effects on liver and kidney function in rats, potentially due to its diverse phytochemicals.

Keywords: Acrylamide, M. oleifera Nanoparticles, liver, kidney toxicity.

Introduction

Acrylamide (ACR) is a dangerous compound found in various foods, including potato chips, and is the main method of exposure to it, as it is produced when carbohydrates are cooked over 180 °C, according to published research into

dietary carcinogens (Annola *et al*., 2008). When ACR enters the body by ingestion, inhalation, or skin contact, it undergoes biotransformation into glycidamide (GA) (Szczerbina *et al*., 2008). Several investigations have shown the risk associated with ACR and its biotransformed metabolite "GA," which raises the risk of cancer in the liver, brain, kidney, intestines, and lungs, among other organs (Capuano and Fogliano, 2011). The body uses two major metabolic pathways for ACR. In one, the cytochrome P450 2E1 (CYP2E1) enzyme system catalyzes an enzymatic process that converts ACR into GA (Rifai *et al*., 2020; Zhao *et al*., 2021). ACR leads to oxidative stress, causing liver damage by increasing lipid peroxidase activity and decreasing antioxidant defense systems (Dobrzynska *et al*., 2004). Moreover, studies have shown that ACR may be changed into glycidamide via the cytochrome P450 route. A DNA-reactive epoxide may then arise as a result of this change in the signal pathway and cellular activity (Tornqvist, 2005). The ACR-intoxicated group in hepatic, renal, and brain homogenates shows a significant increase in malondialdehyde and nitric oxide levels, indicating oxidative stress due to mitochondrial disruption (Liu *et al*., 2015; Bin-Jumah *et al., 2021).*

ACR's high water solubility facilitates quick distribution in organs like the liver and kidney, potentially causing harm due to its ability to form adducts with hemoglobin (Belhadj *et al*., 2019). The rats exposed to ACR had statistically significant increases in their levels of ALT and AST as well as increased lipid peroxidation as compared to the rats in the control and treatment groups (Al Syaad *et al*., 2023). Rat liver slices treated with ACR showed pyknotic Von Kupffer cells, nuclear degeneration hepatocytes, and a dilated central vein. The ACR group had significantly higher AST and ALT enzyme values and elevated MDA and SOD levels in the liver homogenate compared to the control group (El-Sharouny *et al*., 2016). The ACR kidney group experienced severe hydropic degeneration and coagulation necrosis, with high blood flow in interstitial capillaries. After ten days of oral therapy, serum creatinine and urea concentrations significantly increased compared to the control group (Kandemir *et al*., 2020). Reactive carcinogens, or DNA damage from toxic substances (ACR, GA) during DNA replication, are typically responsible for tumor formation in the hormonal and endocrine glands, according to Rice and Wilbourn's 2000 study on mice.

Moringa oleifera (*M. oleifera*) is a traditional medicine plant used for its medicinal properties, including inhibiting pharmacological activities that cause inflammation, allergies, heart disease, seizures, liver protection, hepatitis, kidney stones, anemia, wound healing, and treating conditions like colitis, gonorrhea, hypertension, diabetes, anxiety, diarrhea, and diuretics (Prithiviraj and Sumathy, 2021). As stated by Prakash *et al*. (2007), many research have shown the antioxidant capacity of *M. oleifera* seed extract and leaves as a defense against the damaging effects of free radical attack and oxidative stress. Consequently, the leaves' many therapeutic qualities, including their antibacterial, anti-cancer, anti-diabetic, and anti-inflammatory effects, have been studied (Karishma *et al*., 2019). *M. oleifera* is rich in essential phytochemicals like vitamins, ascorbic acid oxidase, total phenols, polyphenol oxidase, and catalase, which are essential enzymes (Aboulthana *et al*., 2021a). Saleem *et al*. (2023) assert that *M. oleifera's* greater ability to recover increased levels of liver enzymes (ALT, AST, and serum bilirubin) makes it a suitable therapy for hepatotoxicity. *M. oleifera* treatment was shown to have a hypolipidemic effect on the kidneys of diabetic rats, as shown by a reduction in kidney size (Omodanisi *et al*., 2017). Studies suggest that *M. oleifera's* antiproliferative effects may be due to its ability to increase oxidative stress, leading to DNA fragmentation and death in A549 lung cancer cells (Abd-Rabou *et al*., 2017). Remarkably, studies have shown that the addition of silver nanoparticles (Ag-NPs) could increase the antioxidant activity of *M. oleifera* leaf extract, which has a high concentration of phytoconstituents (Aboulthana *et al*., 2021b). Ag-NPs are widely used in various industries like chemistry, medicine, electronics, and catalysis due to their environmental benefits. They are produced using non-toxic substances and stabilized by plant extracts, proteins, enzymes, antioxidants, glycoproteins, flavonoids, terpenes, and tannins, making them a valuable resource in various applications (Ramaswamy *et al*., 2019). The study investigated the oxidative damage caused by ACR on rats' livers and kidneys and the potential protective and therapeutic effects of *M. oleifera* leaf nanoparticles in adult male rats.

Material and Methods

Preparation of Moringa oleifera Extract (*Mo-extract)*

Ten grams of powder and 100 milliliters of distilled water were combined to create the *M. oleifera* extract (Mo-extract). This was mixed to dissolve the powder and then heated for 10 minutes, or until the extracted solution took on a light green hue. The extract was filtered through filter paper and stored at 4 ℃ to preserve it for use as Mo-extract in the future (Nilanjuna *et al*., 2014; Abdel-Rahman *et al*., 2022).

Synthesis of Silver Nanoparticles (Ag-NPs) Carried by Moringa oleifera (Mo-NPs)

190 mL of a 2 mM silver nitrate solution was combined with 10 mL of MO-extract while being continuously stirred as part of the experiment. A dark brown color results from stirring the solution in a magnetic stirrer for four hours at room temperature, then letting it sit in the dark for twenty-four hours. It was allowed to condense into pellets after the solution was centrifuged at 5000 rpm for at least 20 minutes at a constant temperature. Upon discarding the supernatant, the granules were re-dispersed in distilled water and allowed to air dry prior to being preserved for future use (Nilanjuna *et al*., 2014; Abdel-Rahman *et al*., 2022).

Characterization of silver nanoparticles derived from M. oleifera

By our recently published study (Abduljalil *et al*., 2023), *M. oleifera* silver nanoparticles were produced and characterized using an advanced confirmatory process (Transmission Electronic Microscopy and Dynamic Light Scattering (DLS) and Zeta Potential), and the optical characteristics of the silver nanoparticles were measured using an ultraviolet-visible spectrophotometer (UV-VIS), specifically the Jasco V-630 UV-visible spectrophotometer. The measurements were made between 300 and 600 nm (Herbin *et al*., 2022).

Experimental Design

Following their random division into four groups of five rats each, the rats were weighed at around 150 grams each. The groups that were formed were as follows:-

1. Control group (CT): rats received nothing additional to their normal diet.
2. Acrylamide group (ACR): rats were given 50 mg/kg body weight (b.wt.) in their drinking water daily for 3 weeks (LoPachin *et al*., 2006; Gawesh *et al*., 2021).
3. Protection group (Mo-NPs /ACR): rats received 50 mg/kg b.wt. of *M. oleifera* nanoparticles (Mo-NPs) daily for 3 weeks and were given 50 mg/kg b.wt. of acrylamide (ACR) daily for 3 weeks (Malathi *et al*., 2018; Ramaswamy *et al*., 2019).
4. Treatment group (ACR/Mo-NPs): rats were given 50 mg/kg b. wt. of acrylamide (ACR) for 3 weeks, followed by50 mg/kg b.wt. of *M. oleifera* nanoparticles (Mo-NPs) for 3 weeks.

Collection of blood samples

During the conclusion of the experiment, rats were given chloroform anesthesia. Every blood sample was then extracted from the heart using 5 mL syringes. Ethylenediamine tetraacetic acid (EDTA) was added to sterile tubes containing blood samples to assess the activity of the kidney and liver enzymes

Collection of Tissue samples

Following the animal's sacrifice, the liver and kidney tissues were removed, stored in 10% formalin, and then subjected to standard processing procedures before being embedded in paraffin. For microscopic analysis, 5 µm-thick slices were cut and stained with hematoxylin and eosin (H&E) dye (Drury *et al*., 1976). The stained slices were seen using a light microscope and photographed on camera.

Comet assay

The comet assay was conducted according to the protocol of Tice *et al*. (2000). After filling frosted slides with 1% normal-melting agarose, the agarose was wiped from the bottom of the slide. Ten minutes at 4 ℃ were allowed for the slide to harden. Subsequently, 10 µl of whole liver cells were combined with 0.5% low-melting agarose (75 µl, 37 ℃) and applied to the coated surface. The slides were immersed in the prepared cold lysis buffer (100 mM

Na2EDTA, 2.5 M NaCl, 10 mM Tris HCl, pH 10). Before immersing the slides in the lysis solution, the last dosages of 10% DMSO and 1% Triton X-100 were added. After that, the slides in the lysis buffer jar were kept cold all night. After that, the slides were kept for 20 minutes at a pH higher than 13 in an alkaline buffer (1 mM EDTA and 300 mM NaOH) to allow the DNA to unwind. 25 minutes were needed for the electrophoresis at 300 mA and 25 V (~ 0.74 V/cm). The slides were then emptied and given three five-minute cleanings using neutralizing buffer (0.4 M Tris HCl, pH 7.5). The slides were dehydrated for five minutes in pure methanol, and then they were left to air dry at room temperature. The whole procedure was done in dim light to prevent damage to DNA. We looked at the slides under a fluorescence microscope after treating them with a 10% ethidium bromide solution. Using a Leica microscope camera, comet analysis software (Kinetic Imaging, Ltd., Liverpool, UK) was utilized to concurrently take pictures and score 50 cells at a 400x magnification. A variety of endpoints were used to measure DNA damage. The tail length (μm) was used to assess the amount of damage to the DNA that is located distant from the nucleus. By dividing the total intensity of all comet pixels by the intensity of all tail pixels, one may determine the proportion of DNA in the tail. Tail DNA percentage/100 is equal to tail length × tail moment.

Statistical Analysis

SPSS Version 25 was used to conduct the statistical analysis. One-way variance analysis tests (ANOVA) were used to assess each outcome. The findings were presented as mean (M) ± standard deviation (SD) (N=5), with $p<0.05$ regarded as statistically significant.

Results

Characterization of Silver nanoparticles

UV-Visible Spectroscopy

The presence of the silver nanoparticles was shown by characterizing them using UV-visible spectroscopy. Scanning UV-visible spectroscopy between 300 and 600 nm was used to confirm the biogenesis of Ag-NPs. Surface plasmon resonance (SPR) spectroscopy showed a high absorption band at 460 nm when the silver nanoparticles were made using an extract from *M. oleifera* leaves. For the Ag-NPs solution, the absorbance was 430 nm (Fig. 1).

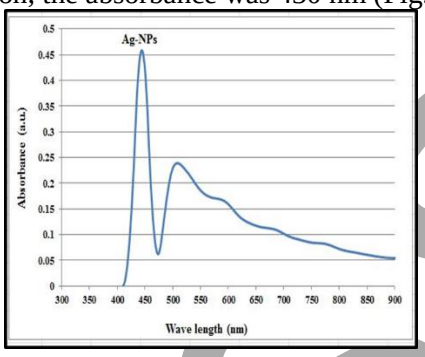

Figure (1): A peak of UV-visible absorption is seen at 430 nm in Ag-NPs derived from *M. oleifera* leaf extract.

Physiological studies (Liver enzyme activities)

Alanine / Aspartate aminotransferase (ALT/AST) enzyme activities

The study found that after three weeks of taking ACR by mouth at a dose of 50 mg/kg b.wt., the average levels of ALT and AST were statistically significantly higher in the ACR group compared to the control group (Table 1). After three weeks of administering *M. oleifera* nanoparticles to rats at a dosage of 50 mg/kg b.wt., the mean ALT and AST values in both the protection and treatment groups decreased significantly compared to those in the ACR group. One-way ANOVA statistical analysis revealed that all groups had an extremely significant difference in the mean values of ALT and AST ($p< 0.000$). In fact, statistical analysis shows that rats that were given *M. oleifera* nanoparticles in both the protection and treatment groups had lower mean ALT and AST activities than rats that were only given ACR ($p< 0.000$).

Superoxide dismutase (SOD U/ml) and Malondialdehyde (MDA U/ml) enzyme activities

Based on the findings of the current study, the mean levels of MDA in the ACR group compared to the control group increased statistically significantly after three weeks of oral administration of ACR at a dosage of 50 mg/kg b.wt, associated with a significant decrease in SOD (Table 1). After administering

M. oleifera nanoparticles to the rats for three weeks at a dosage of 50 mg/kg b.wt., the mean MDA values in the protection and treatment groups decreased significantly, accompanied by a significant increase in the SOD mean value compared to those in the ACR group. One-way ANOVA statistical analysis revealed that all groups had an extremely significant difference in the mean values of SOD and MDA ($p< 0.000$). Statistical analysis shows that rats that were given *M. oleifera* nanoparticles in both protection and treatment groups had lower mean MDA and higher mean SOD activities than rats that were only given ACR ($p< 0.000$).

Physiological studies (Kidney Function)

Creatinine and Urea levels

After three weeks of oral ACR at a dose of 50 mg/kg b.wt., the ACR group showed statistically significant higher average levels of creatinine and urea compared to the control group (Table 1). The mean creatinine and urea levels in both the protection and treatment groups were considerably lower than those in the ACR group during the three weeks of administration of *M. oleifera* nanoparticles to the rats at a dose of 50 mg/kg b.wt. The creatinine and urea levels in each group differed significantly ($p<0.000$), according to a one-way ANOVA statistical analysis. According to statistical analysis, rats that received *M. oleifera* nanoparticles in both protection and treatment groups had lower mean creatinine and urea activity than rats that received ACR alone ($p<0.000$).

Table 1: The mean values of ALT/AST enzymes, SOD, MDA enzyme activities, creatinine, and urea levels in the serum of the rats in all experimental groups.

Parameters	**Groups**				***P* value (ANOVA)**
	CT	**ACR**	**Mo-NPs/ACR**	**ACR/Mo-NPs**	
	Mean ± SD	**Mean ± SD**	**Mean ± SD**	**Mean ± SD**	
ALT (U/L)	42.80±3.49	76.80±5.76 P1=0.000***	51.60±3.64 P1=0.050* P2=0.001***	61.80±4.20 P1=0.001** P2=0.021* P3=0.039*	0.000***
AST (U/L)	196.20±2.38	258.60±2.07 P1=0.000***	219.60±1.51 P1=0.000*** P2=0.000***	234.20±3.76 P1=0.000*** P2=0.000*** P3=0.004**	0.000***
SOD (U/ml)	207.17±2.11	181.10±3.16 P1=0.000***	201.17±1.35 P1=0.013* P2=0.000***	193.06±1.50 P1=0.000*** P2=0.003** P3=0.000***	0.000***
MDA (nmol/ml)	10.28±0.17	20.36±1.10 P1=0.000***	13.28±0.83 P1=0.004** P2=0.000***	16.91±1.23 P1=0.000*** P2=0.019* P3=0.010*	0.000***
Creatinine (mg/dl)	0.68±0.08	2.28±0.26 P1=0.000***	1.24±0.08 P1=0.000*** P2=0.002**	1.72±0.04 P1=0.000*** P2=0.013* P3=0.006**	0.000***
Urea (mg/dl)	37.20±2.20	55.40±2.07 P1=0.000***	46.40±1.14 P1=0.004** P2=0.002**	49.60±1.67 P1=0.000*** P2=0.010* P3=0.351^{NS}	0.000***

The data are presented as Mean ± SD (N = 5 for each group). (NS) Non-significant, (*) Significant, (**) High significant, (***) Extremely significant. P1: compared with control group; P2: compared with ACR group; P3: compared with Mo-NPs/ACR group. CT: control group; ACR: acrylamide group; Mo-NPs/ACR: silver nanoparticles of *M. oleifera* for three weeks, followed by ACR for 3 weeks group and ACR/Mo-NPs: ACR for 3 weeks, followed by silver nanoparticles of *M. oleifera* for three weeks.

Histological studies (Liver Histology)

Histopathological of the liver in the control group

The livers of control rats had normal hepatic tissue structure, devoid of any obvious pathological changes. The hepatocytes are arranged into cords from the central veins to the portal areas, with sinusoids dividing them. Hepatocytes have eosinophilic cytoplasm inside their central vesicular nuclei. Some cells have nuclei that are binucleated. Kupffer cells are found in the blood sinusoids (Fig. 2 A).

Histopathological analysis of the liver in the ACR group

The administration of ACR congested the central vein, and more kupffer cells activated, inflammatory cells invaded, some hepatocytes necrotized, the cytoplasm vacuolates, and the hepatocytes lost their cellular boundaries (Fig. 2 B).

Histopathological analysis of the liver in the protection group (Nanoparticles of M. oleifera for 3 weeks followed by ACR for 3 weeks) (Mo-NPs/ACR)

The liver had normal periportal hepatocytes and less post-translational hypertrophy. However, blood clots were seen in some sinusoids in a section of the liver from rats that had been treated with *M. oleifera* nanoparticles and then ACR (Fig. 2 C).

Histopathological analysis of the liver in the treatment group (ACR for 3 weeks, followed by Nanoparticles of M. oleifera for 3 weeks) (ACR/Mo-NPs)

Rats treated with silver nanoparticles of *M. oleifera* showed fewer histological alterations caused by ACR, and regular placement of hepatocytes in cords reduced the number of inflammatory cells. Hematoxylin and eosin staining revealed normal hepatocytes, with no visible pathological damage (Fig. 2 D).

Histological studies (Kidney Histology)

Histopathological analysis of the kidney in the control group

Kidney tissue slices from control rats showed no obvious pathological changes and had normal renal tissue structure. There were visible normal glomeruli and renal tubules in Bowman's capsule (Fig. 3 A).

Histopathological analysis of the kidney in the ACR group

After ACR injury, the rats' kidneys showed glomeruli shrinkage with Bowman's gap expansion, renal tubule epithelial degradation, and necrosis, as well as inflammatory cell infiltration and bleeding into the renal interstitial space (Fig. 3 B).

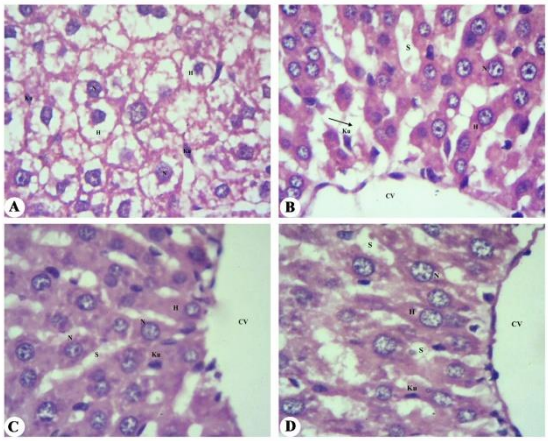

Figure (2): A) A photomicrograph of the rat liver of the control group shows preserved liver architecture. H: hepatocyte; N: nucleus; Ku: kupffer cells; S: sinusoid. B) A photomicrograph of the ACR-treated group's rat liver. Showing the CV: congested central vein; N: nucleus; Ku: kupffer cells; S: sinusoid; black arrow: necrosis. C) A photomicrograph of the rat liver from the protection group. Showing the CV: central vein, H: hepatocyte, N: nucleus, Ku: kupffer cells, S: sinusoid. D) A photomicrograph of the rat liver from the treatment group. Showing the CV: central vein, H: hepatocyte, N: nucleus, Ku: kupffer cells, S: sinusoid. H&E X400.

Histopathological analysis of the kidney in the protection group (Nanoparticles of M. oleifera for 3 weeks followed by ACR for 3 weeks) (Mo-NPs/ACR)

Rats pre-treated with nanoparticles from *M. oleifera* showed less severe histopathological changes caused by ACR, and after three weeks, kidney structures were almost normal. However, a renal infiltrate, dilated renal tubules, and Bowman's gap were visible (Fig. 3 C).

Histopathological analysis of the kidney in the treatment group (ACR for 3 weeks, followed by Nanoparticles of M. oleifera for 3 weeks) (ACR/Mo-NPs)

M. oleifera nanoparticles treatment restored renal architecture with minimal infiltration, revealing intact and normal renal architecture with excellent condition of glomeruli, interstitial tissues, and convoluted tubules, according to histological analysis (Fig. 3 D).

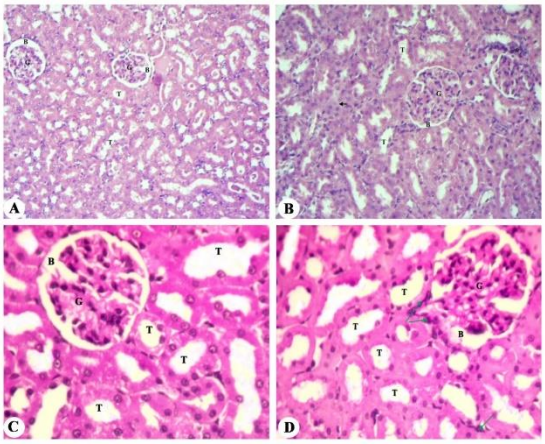

Figure (3): A) A photomicrograph of the rat kidney of the control group shows preserved kidney architecture. G: glomerulus; B: Bowman's capsule; T: renal tubule. B) A photomicrograph of rat kidneys in the ACR group. Showing the G: glomerulus, B: Bowman's capsule, T: renal tubule, green arrow: infiltration, black arrow: tubules' degeneration, *: necrosis, head arrow: interstitial hemorrhage. C) A photomicrograph of the rat kidney from the protection group. Showing the G: glomerulus, B: Bowman's capsule, and T: renal tubules. D) A photomicrograph of the rat kidney from the treatment group. Showing the G: glomerulus, B: Bowman's capsule, T: renal tubules, green arrow: interstitial infiltration. H&E X400.

Genetic studies

Comet assay

Table 2 presents the results of the comet assay after *M. oleifera* nanoparticle treatment and ACR injection. The length of the comet and the percentage of DNA in the tail are the two primary factors used to evaluate DNA damage. The tail DNA percentage and tail length of ACR showed a very substantial rise in a time-dependent way. Furthermore, statistical analysis shows that rats that were given *M. oleifera* nanoparticles in both the protection and treatment groups had decreased tail length, tail DNA percentage, tail moment, and tail olive moment compared to rats that were only given ACR ($P<0.000$). However, there was no statistically significant difference between the rats treated with *M. oleifera* nanoparticles in the protection group and the control group ($P>0.05$). Figures from (Fig. 4 A to D) display the comet morphology of the various groups that were analyzed. The control group had no detectable DNA damage (Grade 0; tail DNA percentage < 5%), according to this analysis. However, ACR results in significantly severe liver DNA damage (Grade 2; tail DNA percentage 20–40%) (Fig. 4 A & B). Because the nucleus had a fluorescent stripe emanating from it and the liver cells had more damaged DNA, it altered the nuclear DNA profile in the ACR group. However, rats in the protection group that were given *M. oleifera* nanoparticles had a significant reduction in DNA damage to their liver cells (Grade 0; tail DNA percentage < 5%) (Fig. 4 C). The rats in the treatment group that were given *M. oleifera* nanoparticles had moderate liver DNA damage (Grade 1; tail DNA percentage 5–20%) (Fig. 4 D).

Table 2: Variation in terms of percentage damage, tail length, tail DNA, tail moment, and tail olive moment after ACR injection and *M. oleifera* nanoparticle therapy.

Groups	**Comet assay**			
	Tail length	**Tail DNA%**	**Tail Moment**	**Tail Olive Moment**
	Mean±SD	**Mean±SD**	**Mean±SD**	**Mean±SD**
Control (CT)	1.83±0.14	12.28±0.69	0.30±0.02	0.79±0.13
Acrylamide (ACR)	5.72±0.24 P1=0.000***	24.01±1.07 P1=0.000***	1.83±0.18 P1=0. 000***	2.21±0.22 P1=0. 000***
Mo-NPs / ACR	2.12±0.17 P1=0.704 NS P2=0. 000***	14.00±0.47 P1=0.017** P2=0. 000***	0.35±0.01 P1=0. 944 NS P2=0. 000***	0.94±0.03 P1=0. 544 NS P2=0. 000***
ACR / Mo-NPs	2.29±0.45 P1=0.247 NS P2=0.000*** P3=0.960NS	18.19±0.87 P1=0.000*** P2=0. 000*** P3=0. 000***	0.48±0.09 P1=0. 070 NS P2=0. 000*** P3=0.349NS	1.10±0.09 P1=0.016** P2=0. 000*** P3=0.422NS
***P* value (ANOVA)**	0.000***	0.000***	0.000***	0.000***

The data are presented as Mean ± SD (N = 5 for each group). (NS) Non-significant, (**) High significant, (***) Extremely significant. P1: compared with control group; P2: compared with ACR group; P3: compared with Mo-NPs/ACR group. CT: control group; ACR: acrylamide group; Mo-NPs/ACR: silver nanoparticles of *M. oleifera* for three weeks, followed by ACR for 3 weeks group and ACR/Mo-NPs: ACR for 3 weeks, followed by silver nanoparticles of *M. oleifera* for three weeks.

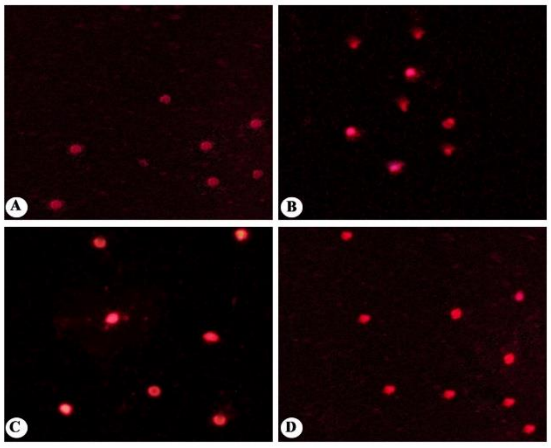

Figure (4): A) Representative photograph of comet morphology displays the pattern of DNA movement in rat liver cells stained with ethidium bromide. Rats in the control group had comet morphology in Grade 0, which indicates minimal harm (tail DNA percentage < 5%). B) Representative photograph of the comet morphology of the ACR group of rats'; Grade 2 indicates medium damage (tail DNA percentage 20–40%) in terms of tail DNA percentage. C) Representative photograph of the comet morphology of rats treated with *M. oleifera* nanoparticles for 3 weeks and followed by ACR for 3 weeks; grade 0 indicates no damage (% tail DNA<5%). D) Representative photograph of the comet morphology of rats treated with ACR for 3 weeks and followed by *M. oleifera* nanoparticles for 3 weeks; grade 1 indicates slight damage (% tail DNA -5–20%).

Discussion

The study investigated the possible protective effects of *M. oleifera* leaf nanoparticles in adult male rats, as well as the oxidative damage that ACR causes to the rats' livers and kidneys. Using UV-visible spectroscopy, the study investigated the structural properties of Ag-NPs, a material employed in silver ion reduction. The formation of Ag-NPs was shown by the nanoparticle peaks falling within the predicted range. The natural extract's surface plasmon resonance (SPR), which has a peak at 430 nm, caused the generated MO Ag-NPs to change color. Additionally, Ag-NPs prepared from *M. oleifera* leaves had UV-Vis spectral peaks at 420, 430, 460.8, and 450 nm (Ilavarashi *et al*., 2019; Abdel-Rahman *et al*., 2022).

Researchers use serum urea and creatinine levels to assess renal health and structural integrity, while they use blood ALT and AST activities to diagnose specific liver disorders (Turk *et al*., 2019). As a result, rats given ACR (50 mg/kg b.wt.) for three weeks in this study showed a significant increase in their ALT and AST enzyme activity levels. The findings are similar to Soliman's (2013) research, which revealed signs of post-ACR intoxication in mouse and rat serum and plasma. Indeed, oral ACR significantly increased ALT and AST levels compared to the healthy control group, with the ACR group's AST higher than control and all other groups (Moustafa, 2023). The study suggests that exposure to ACR may pose potential health risks. *M. oleifera* nanoparticles showed anti-hepatotoxic properties in rats, reducing ALT and AST levels and indicating early improvement in cell membrane integrity. These findings are consistent with those of Saleem *et al*. (2023), who discovered that since *M. oleifera* is more effective at decreasing high levels of hepatocyte enzymes (ALT and AST), it should be utilized as a therapy for hepatotoxicity. The study is similar to Rifai *et al.* (2020) findings, which suggest that *M. olifera* can lower ACR levels in French fries and potentially repair liver damage in ACR-intoxicated animals. The extract may protect the structural integrity of the hepatocyte membrane from reactive oxygen species.

The study revealed that rats given ACR had significantly increased MDA levels while reducing liver SOD levels. The study aligns with Rahbardar *et al* (2021) findings, which showed that ACR significantly increased MDA levels in hepatic cells, while SOD levels decreased in the control group. Moreover, the study agrees with Tomaszewska *et al.* (2022) findings, showing higher blood MDA and lower blood SOD levels in offspring from the long-exposure ACR group. *M. oleifera* nanoparticles improved the integrity of the liver cell membrane and had anti-hepatotoxic effects by decreasing MDA levels. In line with earlier research by Hamza (2010), they also raised SOD levels in rats. This suggests that the antioxidant properties of moringa seed extract may offer protection against fibrosis and carbon tetrachloride toxicity. Additionally, the extract was found to be able to stop liver MDA levels from rising and SOD activity from declining. In addition, El-bakry *et al*. (2016) discovered that treatment with *M. oleifera* leaf extract decreased MDA levels, enzyme activity, and the activation of antioxidant parameters.

The levels of urea and creatinine increased significantly in rats given ACR compared to rats

not receiving treatment. Research indicates that rats intoxicated with ACR have significantly higher blood levels of renal function indicators like urea and creatinine compared to those with normal renal function (Bin-Jumah *et al*., 2021). The study confirms a previous study by Sun *et al*. (2020), which showed significantly higher blood levels of urea and creatinine in rats intoxicated with ACR compared to control rats. The results of the study demonstrated that *M. oleifera's* nanoparticles considerably decreased urea and creatinine levels, hence supporting their common use in conventional medicine. *M. oleifera*, a plant known for its kidney-protective properties, has been utilized in various treatments such as diuretics, hypotension, and diabetes. (Prithiviraj and Sumathy, 2021). According to El Rabey *et al*. (2023), silymarin and Ag-NPs significantly protect the kidneys from changes caused by carbon tetrachloride, whereas vanillic acid only slightly does.

The study revealed that rats treated with ACR exhibited significant liver and kidney damage, indicating inflammatory alterations and structural deformation in these organs. ACR therapy causes central venous blockage, hepatocyte apoptosis, vacuolated cytoplasm, cellular loss, elevated kupffer cell activity, and inflammatory cell movement. The present study confirms the findings of Mahmood *et al*. (2015) study, which found that rats given ACR exhibited liver deterioration, clogged blood vessels, and inflammatory cell infiltration, while high-dose mice showed significant infiltration and blocked blood vessels. Additionally, this is consistent with the results of El-Sharouny *et al*. (2016), which showed cytoplasmic enlargement, nuclear degeneration, and dilated central veins in liver sections. *M. oleifera* nanoparticles may mitigate ACR-induced histological changes in rats by reducing epithelial hypertrophy, preventing sinusoidal blood clot formation, and maintaining normal liver periportal hepatocytes. This is in line with the finding of Dharmendra *et al*. (2014) that stable blood total bilirubin levels after injection of MO-extract signal improved hepatocyte cell activity. This is in line with the results of El-bakry *et al*. (2016), who found that MO-extract improves hepato-fatty degeneration, inflammation-related cell infiltration, and liver structural disruption.

Histological examination revealed kidney congestion, bleeding, glomeruli atrophy, and tubule epithelium degeneration, consistent with Sun *et al*. (2020) findings of kidney fragmentation, hemorrhage, glomerular congestion, tubular necrosis, cell swelling, and mononuclear cell infiltration. According to Kandemir *et al*. (2020), coagulation necrosis in the tubular epithelium causes enormous hyperemia and severe hydropic degeneration in the kidneys for those with ACR. According to the findings, administering *M. oleifera* nanoparticles to rats prevented renal alterations caused by ACR and restored normal kidney structure. This is in line with the results of Saleh (2018), who demonstrated that rats administered MO-extract exhibited almost normal kidney structure and collagen fiber distribution, along with low tubule epithelial cell lining deterioration. Moreover, Akinrinde *et al*. (2020) reported improved renal histology, fewer glomerular lesions, less inflammation, and improved endothelial, glomerular, tubular, and interstitial scoring system indices. Additionally, the extract demonstrated tissue-protective properties that maintained glomeruli and guaranteed urine excretion.

The study evaluates the genetic damage caused by ACR therapy using tail length and tail DNA percentage. The results demonstrate that, over time, ACR injection dramatically increases tail length and DNA percentage. Not all treatment groups exhibited Grades 3 and 4, since the ACR group had substantial DNA damage (Grade 2). These results imply that ACR is genotoxic at the injected dose and that the liver is an important target organ. The study aligns with Ansar *et al*. (2016) findings, showing quercetin reduces liver damage in the ACR + quercetin group, while ACR enhances liver damage, and no significant difference was observed between the quercetin + ACR group and the control group. Furthermore, Dobrzyńska (2007) investigation discovered that delivering 100 mg/kg bw ACR increased DNA migration across many organs, with liver cells exhibiting the greatest reaction. Mice subjected to 75–125 mg/kg bw ACR showed similarly elevated DNA damage, with ACR causing the most damage. When both were administered, liver cells suffered similar damage. *M. oleifera* nanoparticle therapy for three weeks can repair DNA damage (Grade 0) in the protection group, but rats in the treatment group, which was treated with ACR and followed by *M. oleifera* nanoparticles for three weeks (Grade 1), showed slight damage. The study (El-bakry *et al*., 2016) found that rats given *M. oleifera* extract had improved livers

after poisoning because it increased the amount of hepato-fatty degeneration, altered the liver architecture, and allowed inflammatory cells to enter the liver. According to Sikder *et al*. (2013), the extract protected DNA from oxidative stress-induced damage by lowering LPO levels by 30%, stopping comet formation and hydroxyl radical damage, and lowering topoisomerase I activity. These findings raise the possibility that humans could consume the extract to prevent oxidative DNA and cell damage.

Conclusion

The study's results show that, *M. oleifera* nanoparticles have shown enhanced protection against acrylamide's effects on liver and kidney function in rats, as well as liver DNA damage, possibly due to its diverse phytochemicals.

References

Abdel-Rahman, L. H., Al-Farhan, B. S., El-ezz, A., Sayed, A. E., Zikry, M. M., & Abu-Dief, A. M. (2022). Green Biogenic Synthesis of Silver Nanoparticles Using Aqueous Extract of Moringa Oleifera: Access to a Powerful Antimicrobial, Anticancer, Pesticidal and Catalytic Agents. Journal of Inorganic and Organometallic Polymers and Materials, 32(4):1422-1435.

Abduljalil, A. H. Y., Elbakry, K., Omar, N. A., & Deef, L. (2023). Protective Effects of Silver Nanoparticles of Moringa Oleifera Leaves against Acrylamide-Induced Blood Toxicity in Rats. Scientific Journal for Damietta Faculty of Science, 12(2), 66-75.

Abd-Rabou, A. A., Abdalla, A. M., Ali, N. A., & Zoheir, K. M. (2017). Moringa oleifera root induces cancer apoptosis more effectively than leave nanocomposites and its free counterpart. Asian Pacific journal of cancer prevention: APJCP, 18(8), 2141.

Aboulthana, W. M., Shousha, W. G., Essawy, E. A. R., Saleh, M. H., & Salama, A. H. (2021b). Assessment of the Anti-Cancer Efficiency of Silver Moringa oleifera Leaves Nano-extract against Colon Cancer Induced Chemically in Rats. Asian Pacific Journal of Cancer Prevention: APJCP, 22(10): 3267.

Aboulthana, W. M., Youssef, A. M., Seif, M. M., Osman, N. M., Sahu, R. K., Ismael, M., & Omar, N. I. (2021a). Comparative study between Croton tiglium seeds and Moringa oleifera leaves extracts, after incorporating silver nanoparticles, on murine brains. Egyptian Journal of Chemistry, 64(4):1709-1731.

Akinrinde, A. S., Oduwole, O., Akinrinmade, F. J., & Bolaji-Alabi, F. B. (2020). Nephroprotective effect of methanol extract of Moringa oleifera leaves on acute kidney injury induced by ischemia-reperfusion in rats. African health sciences, 20(3), 1382-1396.

Al Syaad, K. M., Al-Doaiss, A. A., Ahmed, A. E., El-Mekkawy, H., Abdelrahman, M., El-Mansi, A. A., & Ali, M. E. (2023). The abrogative effect of propolis on acrylamide-induced toxicity in male albino rats: Histological study. Open Chemistry, 21(1), 1–11.

Annola, K., Karttunen, V., Keski-Rahkonen, P., Myllynen, P., Segerbäck, D., Heinonen, S., & Vähäkangas, K. (2008). Transplacental transfer of acrylamide and glycidamide are comparable to that of antipyrine in perfused human placenta. Toxicology letters, 182(1-3), 50-56.

Ansar, S., Siddiqi, N. J., Zargar, S., Ganaie, M. A., & Abudawood, M. (2016). Hepatoprotective effect of Quercetin supplementation against Acrylamide-induced DNA damage in wistar rats. BMC complementary and alternative medicine, 16(1), 1-5.

Belhadj Benziane, A., Dilmi Bouras, A., Mezaini, A., Belhadri, A., & Benali, M. (2019). Effect of oral exposure to acrylamide on biochemical and hematologic parameters in Wistar rats. Drug and chemical toxicology, 42(2), 157-166.

Bin-Jumah, M. N., Al-Huqail, A. A., Abdelnaeim, N., Kamel, M., Fouda, M. M., Abulmeaty, M. M., & Abdel-Daim, M. M. (2021). Potential protective effects of Spirulina platensis on liver, kidney, and brain acrylamide toxicity in rats. Environmental Science and Pollution Research, 28, 26653-26663.

Capuano E, Fogliano V. (2011). Acrylamide and 5-hydroxymethylfurfural (Hmf): a review on metabolism, toxicity, occurrence in food and mitigation strategies. LWT-food science and technology, 44:793–810.

Dharmendra, S., Vrat, A. P., Prakash, A. V., & Radhey, S. G. (2014). Evaluation of Antioxidant and Hepatoprotective Activities of Moringa oleifera Lam. Leaves in Carbon Tetrachloride-Intoxicated Rats. Antioxidants, 3, 569-591.

Dobrzyńska, I., Sniecińska, A., Skrzydlewska, E., & Figaszewski, Z. (2004). Green tea modulation of the biochemical and electric properties of rat liver cells that were affected by ethanol and aging. Cellular & molecular biology letters, 9(4A), 709-721.

Dobrzyńska, M. M. (2007). Assessment of DNA damage in multiple organs from mice exposed to X-rays or acrylamide or a combination of both

using the comet assay. in vivo, 21(4), 657-662.

Drury RA, Wallington EA, & Cancerson R. (1976). Carlton's Histopathological Techniques, Oxford University Press, Oxford, UK, 4th edition.

El Rabey, H. A., Alamri, E. S., Alzahrani, O. R., Salah, N. M., Attia, E. S., & Rezk, S. M. (2023). Silymarin and Vanillic Acid Silver Nanoparticles Alleviate the Carbon Tetrachloride-Induced Nephrotoxicity in Male Rats. International Journal of Polymer Science, 10, 1 - 11.

El-bakry, K., Toson, E. S., Serag, M., & Aboser, M. (2016). Hepatoprotective effect of Moringa oleifera leaves extract against carbon tetrachloride-induced liver damage in rats. World Journal of Pharmacy and Pharmaceutical Sciences, 5(5), 76-89.

El-Sharouny, S. H., El-Enein, R. A., ArsaniosSF, S. T. M., & Bayoumy, A. H. (2016). Acrylamide induced liver toxicity and the possible protective role of vitamin E in adult male albino rat: histological, biochemical and histochemical study. The Egypt Journal of Medical Sciences, 37(2), 727-746.

Gawesh, E. S., Hamdey, E. S., Abdelreheem Elshoura, A. I., & Abbas, M. A. (2021). Protective Effect of Cinnamon and Ginger on Acrylamide Induced Hepatotoxicity in Adult Male Albino Rats. International Journal of Medical Arts, 3(1), 1136-1144.

Hamza, A. A. (2010). Ameliorative effects of Moringa oleifera Lam seed extract on liver fibrosis in rats. Food and Chemical Toxicology, 48(1), 345-355.

Herbin, H. B., Aravind, M., Amalanathan, M., Mary, M. S. M., Lenin, M. M., Parvathiraja, C., & Islam, M. A. (2022). Synthesis of silver nanoparticles using syzygium malaccense fruit extract and evaluation of their catalytic activity and antibacterial properties. Journal of Inorganic and Organometallic Polymers and Materials, 32(3),1103–1115

Ilavarashi, P., Rani, N., Velusamy, R., Raja, M. J., & Ponnudurai, G. (2019). In-vitro anthelmintic evaluation of synthesized silver nanoparticles of Moringa oleifera seeds against strongyle nematode of small ruminants. Journal of Pharmacognosy and Phytochemistry, 8(6), 2116-2121.

Kandemir, F. M., Yıldırım, S., Kucukler, S., Caglayan, C., Darendelioğlu, E., & Dortbudak, M. B. (2020). Protective effects of morin against acrylamide-induced hepatotoxicity and nephrotoxicity: A multi-biomarker approach. Food and Chemical Toxicology, 138, 111190.

Karishma, S., Lakshmi, K., Tony, D. E., Babu, A. N., & Nadendla, R. R. (2019). Pharmacological evaluation of leaf extract of Terminalia bellerica with Moringa oleifera for its synergistic action on anti-diabetic activity and anti-inflammatory activity in rats. Research Journal of Pharmacy and Technology, 12(3), 1181-1184.

Liu, Z., Song, G., Zou, C., Liu, G., Wu, W., Yuan, T., & Liu, X. (2015). Acrylamide induces mitochondrial dysfunction and apoptosis in BV-2 microglial cells. Free Radical Biology and Medicine, 84, 42-53.

LoPachin, R. M., Barber, D. S., He, D., & Das, S. (2006). Acrylamide inhibits dopamine uptake in rat striatal synaptic vesicles. Toxicological Sciences, 89(1), 224-234.

Mahmood, S. A., Amin, K. A., & Salih, S. F. (2015). Effect of acrylamide on liver and kidneys in albino wistar rats. International Journal of Current Microbiology and Applied Sciences, 4(5), 434-44.

Malathi, R., Chandrasekar, S., & Sivakumar, D. (2018). Assessment of toxicity study of ethanolic extract and synthesized silver nanoparticles of Moringa concanensis Nimmo leaves using wister albino rats. International Journal of Current Research in Life Sciences, 7(03):1250-1254.

Moustafa, S. M. (2023). Study the Possible Protective Effect of Saffron Extract on Induced Rats Toxicity by Acrylamide. Egyptian Journal of Nutrition and Health, 17(2), 51-69.

Nilanjuna, G., Samrat, P., & Piyali, B. (2014). Silver nanoparticles of Moringa oleifera–green synthesis, characterisation and its antimicrobial efficacy. Journal of Drug Delivery and Therapeutics, (11): 20-25.

Omodanisi, E. I., Aboua, Y. G., & Oguntibeju, O. O. (2017). Assessment of the anti-hyperglycaemic, anti-inflammatory and antioxidant activities of the methanol extract of Moringa oleifera in diabetes-induced nephrotoxic male wistar rats. Molecules, 22(4), 439.

Prakash, D., Singh, B. N., & Upadhyay, G. (2007). Antioxidant and free radical scavenging activities of phenols from onion (Allium cepa). Food chemistry, 102(4):1389-1393.

Prithiviraj, E., & Sumathy, G. (2021). A Review on Pharmacological properties of Moringa Oligofera. nveo-natural volatiles & essential oils journal| nveo, 340-355.

Rahbardar, M. G., Farmad, H. C., Hosseinzadeh, H., & Mehri, S. (2021). Protective effects of selenium on acrylamide-induced neurotoxicity and hepatotoxicity in rats. Iranian Journal of Basic Medical Sciences, 24(8), 1041.

Ramaswamy, M., Solaimuthu, C., & Duraikannu, S. (2019). Antiarthritic activity of synthesized silver nanoparticles from aqueous extract of Moringa concanensis Nimmo leaves against FCA induced rheumatic arthritis in rats. Journal of Drug Delivery and Therapeutics, 9(3): 66-75.

Rice, J. M., & Wilbourn, J. D. (2000). Tumors of the nervous system in carcinogenic hazard identification. Toxicologic pathology, 28(1), 202-214.

Rifai, L., Mohammad, M., Raafat, K., & Saleh, F. A. (2020). In Vitro and In Vivo Evaluation of the Protective Potential of Moringa oleifera Against Dietary Acrylamide-induced Toxicity. The Open Medicinal Chemistry Journal, 14(1):26-34.

Saleem, I., Akbar, J., Munir, A., uz Zaman, M. Q., Hussain, A., Lodhi, A. U. S., & Hafeez, K. (2023). Hepatoprotective Properties and Quality Assessment of Two Medicinal Plants: Moringa Oleifera and Curcuma Longa. Journal of Xi'an Shiyou University, Natural Science Edition, 19 (8), 68-80.

Saleh, A. S. (2018). Evaluation of hepatorenal protective activity of Moringa oleifera on histological and biochemical parameters in cadmium intoxicated rats. Toxin Reviews, 10, 8–1.

Sikder, K., Sinha, M., Das, N., Das, D., Datta, S., & Dey, S. (2013): Moringa oleifera Leaf extract prevents in vitro oxidative DNA damage. Asian Journal of Pharmaceutical and Clinical Research, 6(2), 157-161.

Soliman, G. Z. (2013). Protective effect of Solanum nigrum, vitamin C or melatonin on the toxic effect of acrylamide on rats. Journal of Pharmaceutical and Biological Sciences, 5, 47-54.

Sun, R., Chen, W., Cao, X., Guo, J., & Wang, J. (2020). Protective effect of curcumin on acrylamide-induced hepatic and renal impairment in rats: Involvement of CYP2E1. Natural Product Communications, 15(3), 1934578X20910548.

Szczerbina, T., Banach, Z., Tylko, G., & Pyza, E. (2008). Toxic effects of acrylamide on survival, development and haemocytes of Musca domestica. Food and chemical toxicology, 46(7), 2316-2319.

Tice, R. R., Agurell, E., Anderson, D., Burlinson, B., Hartmann, A., Kobayashi, H., & Sasaki, Y. F. (2000). Single cell gel/comet assay: guidelines for in vitro and in vivo genetic toxicology testing. Environmental and molecular mutagenesis, 35(3), 206-221.

Tomaszewska, E., Muszyński, S., Świetlicka, I., Wojtysiak, D., Dobrowolski, P., Arciszewski, M. B., & Mielnik-Błaszczak, M. (2022). Prenatal acrylamide exposure results in time-dependent changes in liver function and basal hematological, and oxidative parameters in weaned Wistar rats. Scientific Reports, 12(1), 14882.

Tornqvist, M. (2005). Acrylamide in food: the discovery and its implications. Advances in experimental medicine and biology, 561, 1.

Turk, E., Kandemir, F. M., Yildirim, S., Caglayan, C., Kucukler, S., & Kuzu, M. (2019). Protective effect of hesperidin on sodium arsenite-induced nephrotoxicity and hepatotoxicity in rats. Biological trace element research, 189, 95-108.

Zhao, S., Zhong, H., Geng, C., Xue, H., Wang, C., Sun, W., & Jiang, P. (2021). Comprehensive analysis of metabolic changes in rats exposed to acrylamide. Environmental Pollution, 287, 117591.

الملخص العربي

عنوان البحث: : التأثير الوقائي والعلاجي للجسيمات النانووية لأوراق المورينجا أوليفيرا ضد السمية الكبدية والكلوية الناجمة عن مادة الأكريلاميد في ذكور الجرذان البالغة

قدري البكري[١]، ناهد عمر[١]، لمياء ضيف[١]، شيرين فهمي[١]، عبدالله يعقوب*[٢]

[١] قسم علم الحيوان – كلية العلوم – جامعة دمياط.
[٢] قسم علم الحيوان – كلية العلوم – جامعة سبها – سبها - ليبيا.

بحثت الدراسة في تأثيرات مادة الأكريلاميد على الكبد والكلى في الجرذان والخصائص الوقائية والعلاجية المحتملة للجسيمات النانووية لأوراق المورينجا أوليفيرا. تم إنتاج جسيمات الفضة النانووية لأوراق المورينجا أوليفيرا وفحصها باستخدام جهاز التحليل الطيفي للأشعة فوق البنفسجية والمرئية. تم تقسيم ٢٠ جرذًا من الذكور البالغين عشوائيا إلى أربع مجموعات: ١- المجموعة الضابطة ؛ ٢- مجموعة الأكريلاميد: تلقت الفئران الأكريلاميد بحوالي ٥٠ ملغم/كغم من وزن الجسم في مياه الشرب لمدة ٣ أسابيع؛ ٣- مجموعة الحماية: تلقت الفئران ٥٠ ملغم/كغم من وزن الجسم من الجسيمات النانووية لاوراق المورينجا أوليفيرا يوميًا لمدة ٣ أسابيع وبعد ذلك تم إعطاؤها ٥٠ ملغم/كغم من وزن الجسم من مادة الأكريلاميد يوميًا لمدة ٣ أسابيع؛ ٤- مجموعة العلاج: أعطيت الفئران ٥٠ ملغم/كغم من وزن الجسم من الأكريلاميد لمدة ٣ أسابيع وبعد ذلك تم إعطاؤها الجسيمات النانووية لاوراق المورينجا أوليفيرا لمدة ٣ أسابيع. لإجراء التحاليل الفسيولوجية والنسيجية، تم الحصول على عينات الدم والأنسجة، وتم استخدام فحص المذنب

((comet assay لتحديد مقدار تلف الحمض النووي في خلايا أنسجة الكبد. أدى العلاج بالأكريلاميد إلى زيادة ارتفاع مستويات مالونديالدهيد MDA، والكرياتينين، واليوريا، و الألنين أمينو ترانسفيريز ALT، و وأسبارتيت أمينو ترانسفيريز AST، مع تقليل انخفاض مستوي إنزيم السوبر أوكسيد دسميوتيز .SODبينما أدى العلاج بالجسيمات النانووية للمورينجا أوليفيرا إلى زيادة نشاط إنزيم SOD وتقليل التأثيرات الضارة للأكريلاميد على مستويات هذه الأنزيمات. الفئران المصابة بالأكريلاميد والتي عولجت بالجسيمات النانووية للمورينجا أوليفيرا أظهرت تحسناً ملحوظا بالنسبة للتشوهات النسيجية في الكبد والكليتين , وشوهد تلف أكبر في الحمض النووي في خلايا الكبد في مجموعة الأكريلاميد بينما تكون المعالجة بالجسيمات النانووية للمورينجا أوليفيرا قد أصلحت هذا الضرر الناتج في الخلايا الكبدية للمجموعات الأخرى. وكشف الدراسة أن الجسيمات النانووية للمورينجا أوليفيرا توفر حماية معززة وقدرة علاجية ضد تأثيرات مادة الأكريلاميد على وظائف الكبد والكلى لدى الفئران، وربما يرجع ذلك إلى المواد الكيميائية النباتية المتنوعة والمضادة للأكسدة الموجودة بها.